Charging and aggregation behavior of silica particles in the presence of lysozymes

doi: 10.1007/s00396-017-4226-2

Charging and Aggregation Behavior of Silica Particles in the Presence of Lysozymes

Yi Huang[1], Atsushi Yamaguchi[1], Tien Duc Pham[2], Motoyoshi Kobayashi[3]

Abstract To gain insight into the colloidal stability in the presence of proteins, we measured the electrophoretic mobility and aggregation rate constant of silica particles coated with lysozymes, and the adsorbed amount of lysozymes on the silica. We also examined model analyses, which are based on the Derjaguin, Landau, Verwey, Overbeek theory with the effect of charge heterogeneity, to discuss the aggregation of lysozyme-coated silica. Our results show that lysozymes enhance the aggregation of silica when the lysozyme-coated silica is near the isoelectric point. When the adsorbed amount of lysozyme is low, the effect of charge-patch attractive force promotes the aggregation of silica. The effect of charge heterogeneity weakens with the increase of adsorbed amount of lysozyme. Our model which takes account of the effect of charge heterogeneity can capture the trend of the aggregation of silica in the presence of lysozyme qualitatively, but there are also large quantitative discrepancies between the theoretical prediction and experimental results. Further improvement is required to describe realistic charge heterogeneity and the effect of the surface coverage of lysozyme on the silica.

Key words Lysozyme, Electrophoretic mobility, Aggregation, Non-DLVO interactions, Charge patch

Motoyoshi Kobayashi	kobayashi.moto.fp@u.tsukuba.ac.jp
Yi Huang	s1621140@u.tsukuba.ac.jp
Atsushi Yamaguchi	s1730266@u.tsukuba.ac.jp
Tien Duc Pham	tienduchphn@gmail.com

1 Graduate School of Life and Environmental Sciences, University of Tsukuba, 1-1-1 Tennoudai, Tsukuba, Ibaraki 305-8572, Japan

2 Faculty of Chemistry, Hanoi University of Science, Vietnam National University, Hanoi, 19 Le Thanh Tong, Hoan Kiem, Hanoi 10000, Vietnam

3 Faculty of Life and Environmental Sciences, University of Tsukuba, 1-1-1 Tennoudai, Tsukuba, Ibaraki 305-8572, Japan

1. Introduction

Colloidal silica and silicate particles are widely encountered in food, cosmetics, and medical industries and also in natural environments [1, 2]. In some cases, colloidal suspensions contain proteins, which are adsorbed on colloidal particles. The adsorption of proteins changes the surface characteristics of colloidal particles, especially the charge state and thus may induce the aggregation of the particles. The adsorption and aggregation influence the quality of products and the fate of substances. Therefore, it is important to understand the adsorption and aggregation behaviors in the mixture of proteins and colloidal silica particles.

Aggregation and dispersion of colloidal particles are usually discussed on the basis of the Derjaguin, Landau, Verwey, and Overbeek (DLVO) theory [3, 4]. According to the DLVO theory, the aggregation behavior of colloidal particles is determined by a repulsive electrical double layer force and the attractive van der Waals force. When the net charge of colloidal particles is close to zero, the repulsive electrical force disappears and the particles aggregate if attractive forces are not counteracted by other repulsive forces. We call this case charge neutralization. The charge neutralization of colloidal particles is practically induced by the adsorption of oppositely charged substances such as polyelectrolytes, multivalent ions, surfactants, and proteins [5–9]. The charge neutralization is usually confirmed as a point of zero zeta potential, where the electrophoretic mobility or zeta potential of particles coated with oppositely charged substances becomes zero. The aggregation rate is usually the fastest near the point of zero zeta potential and slower at conditions far away from the point of zero zeta potential.

The DLVO theory cannot always explain the aggregation behavior of colloidal particles. Bharti et al. [10] observed that silica particles coated with lysozymes aggregate at the point of zero zeta potential. However, Lerche et al. [11] indicated that the particles aggregate despite the absolute value of zeta potential of lysozyme-coated silica is quite high. As a common point, however, they did not measure the aggregation rate constant. Therefore, we cannot evaluate the difference with DLVO theory as shown by previous studies [7, 9, 12]. Kobayashi et al. [12] measured the aggregation rate of bare silica particles and showed that bare silica particles do not aggregate despite the absolute value of zeta potential of silica is low at low pH. They attribute this to the existence of ‘gel-like or hairy layer’ on the silica surface, which provides the steric stabilization. There are also studies [13–15] considering the diffuse layer potential on each particle is not uniform but is normally distributed. With the distribution of diffuse layer potential, the particles are easier to aggregate. They also gave a theoretical model to calculate the aggregation rate constant by which weak dependence of the rate on parameters such as pH and salt concentration is described. Lin et al. [6] showed that stability ratio of sulfate latex particles has a weak dependence on the concentration of cationic dendrimers below the point of zero zeta potential. This study showed that there were electrical attractive forces between charged patches and bare particle surface, and the electrical attractive forces contributed to the aggregation. They described the mechanism qualitatively but they did not give any quantitative model. Through the previous studies with polyelectrolytes and surfactants, the existence of charge-patch forces and steric repulsive forces are discussed. However, it is still unknown that if similar mechanisms work in protein-silica system. Also, models with the distribution

of surface potential have not been applied to the aggregation rate constant in protein-silica system.

Therefore, to improve our understanding on the aggregation of colloids with proteins and the effect of charge heterogeneity, we carried out the measurements of electrophoretic mobility and aggregation rate of silica particles covered with lysozymes and also the adsorption of lysozymes to silica particles. Since the absolute aggregation rate of lysozyme-coated silica with the characterization of adsorption and mobility is scarce, our experimental results are useful and novel. We also analyzed the aggregation rate constant with the classic DLVO theory and the models which take account of the effect of the distribution of diffuse layer potential and the charge heterogeneity.

2. Experiment

2.1 Materials

Colloidal silica particles (KEP-30, Lot No. 3A15) of spherical shape were purchased from Nippon Shokubai. The average diameter of the particles is 302 ± 20 nm determined from transmission electron microscope (TEM) measurements for 800 particles. The density of silica is about 2.2 g/cm^3. The silica particles were heated at 800 ℃ for 24 hours before using to reduce the effect of pores of the particles [16].

Hen egg-white lysozymes from Sigma-Aldrich (L6876) were used as model proteins. The lysozyme has a shape of spheroid with lengths of 3 nm, 3 nm, and 4.5 nm, and the molecular weight is 14.3 kDa. The information of size and charge of lysozyme can be found from some previous studies [17–21]. According to Bharti et al. [22], below pH 8.3, adsorbed lysozymes do not form multilayer on silica surface in their adsorption process. The lysozyme has an isoelectric point around pH 10 [23]. Below pH 10, the lysozyme is positively charged.

Deionized water (Elix Advantage 5, Millipore), with electric conductivity about 0.07 μS/cm, was used for the preparation of all the solutions and suspensions. KCl was used to control the ionic strength. And HCl and KOH solutions were used to control the pH to 5 and 7. All experiments were conducted ~~in~~ at room temperature (20 ℃).

2.2 Measurement of electrophoretic mobility

The electrophoretic mobility of the silica coated with lysozymes was measured to evaluate the zeta potential. We prepared the silica suspension with the particle concentration of 0.1 g/L. The concentration of KCl was set to 1 mM or 10 mM. The dose of lysozyme was varied to change the mass ratio of lysozyme to silica. The experiments were carried out at pH 5 or 7 to ensure that the silica was negatively charged and the lysozyme was positively charged. HCl and KOH solutions were used to adjust pH. The electrophoretic mobility was measured by an electrophoretic light scattering technique with Zeta Sizer Nano ZS (Malvern). The zeta potential is calculated with Smoluchowski's formula, Eq. (5) [24]. However, at pH 7 and the KCl concentration of 1 mM, a relaxation effect cannot be ignored. Therefore, the zeta potential is calculated with Ohshima's formula, Eq. (6) [25].

The electrophoretic mobility of the lysozyme was also measured. We prepared the lysozyme solution

with the concentration of 5 g/L. The concentration of KCl was set to 1 mM or 10 mM. pH was set to 5 and 7. The electrophoretic mobility was measured by an electrophoretic light scattering technique with Zeta Sizer Nano ZS (Malvern).

2.3 Measurement of adsorbed amount

The adsorbed amounts of the lysozymes on the silica particles were measured at the silica concentration of 50 g/L. The mass ratio of lysozyme to silica was changed from 0 to 0.03 g/g. The KCl concentrations were varied from 1 to 10 mM. The suspension pH was set to 5 or 7 with HCl and KOH solutions. The mixed suspensions of silica particles and lysozymes were shaken for 24 hours with a shaker (EYELA Multi Shaker MMS, Tokyo Rikakikai CO., LTD.) to provide sufficient time for the adsorption.

After the shaking, suspensions with different composition were centrifuged at 20630g and around the room temperature (20 ℃) for 5 min with a centrifuge machine (3520, Kubota). The UV absorption (at a wavelength of 280 nm) of the supernatant obtained by the centrifugation was measured by a double beam spectrophotometer UV-1650PC (Shimadzu) to obtain the concentration of lysozyme by using the standard calibration curve of absorbance as a function of lysozyme concentrations. The adsorbed amounts were calculated from the difference between lysozyme concentrations before and after the adsorption. Quartz cells were used in UV absorbance measurements.

2.4 Measurement of aggregation rate constant

Brownian aggregation rate constant was calculated from the temporal change of absorbance of the silica suspension at a wavelength of 450 nm. The absorbance was measured by a spectrophotometer (U-1800, Hitachi). All the cells used in the present experiments were immersed in 0.1 M HCl, 0.1 M KOH, and pure water for 2 hours, respectively. After cleaning, the cells were extensively rinsed with pure water, dried in air, and stored in covered containers to avoid dust. To ensure that the experiments were done in the initial stages, the rate was taken within the coagulation time of half-life $t_{1/2}$, which is the time required for reducing the number of particles to the half. The $t_{1/2}$ is defined by

$$t_{1/2} = \frac{3\eta}{4k_{\mathrm{B}}Tn_0} \tag{1}$$

where η and k_{B} are the viscosity and the Boltzmann constant, *T* is the temperature, and the *T* is 293 K in this study, n_0 is the particle number concentration

$$n_0 = \frac{w_{Si}}{\frac{4}{3}\pi a^3 \rho} \tag{2}$$

where w_{Si}, a and ρ are the concentration of silica, the radius of particles and the density of silica, respectively [26–28]. In this study, all experiments were done with 0.1 g/L silica suspension, so the $t_{1/2}$ is about 58 s. Therefore, the data of initial 10 s were used in the calculation for the fastest rate. For slower rates, data of initial 600 s were used because the slow aggregation rate constant is much smaller than the

fastest rate.

First, we measured the temporal change of the absorbance of the suspension due to aggregation without lysozymes as a function of KCl. This measurement was carried out to confirm the critical coagulation concentration (CCC) and the fastest aggregation rate at pH 5 or 7. Above the CCC, the aggregation rate is mainly determined by the van der Waals force and the frequency of diffusional collision. Then, we measured the temporal variation of the absorbance as a function of lysozyme dose at the constant KCl concentration of 1 mM or 10 mM. Immediately after the lysozyme solution was added to the silica suspension, the measurement was started. We performed a preliminary experiment to confirm the time to reach the equilibrium of lysozyme adsorption. We measured the zeta potential of the mixture of lysozyme and silica immediately after the mixing and 24 hours after the mixing, and we found there are no obvious differences in zeta potential between these two situations. Therefore, we consider the adsorption of lysozyme is rapid enough to reach the equilibrium. The aggregation rate constant of silica *k* can be calculated by

$$k = \frac{1}{n_0}\left(\frac{d\tau}{dt}\right)\frac{1}{\tau_0}\frac{1}{F} \tag{3}$$

where turbidity τ can be obtained from the absorbance. $\frac{d\tau}{dt}$ is the initial rate of turbidity change and the τ_0 is the initial turbidity. *F* is the optical factor of the silica particles and defined by

$$F = \frac{C_2}{2C_1} - 1 \tag{4}$$

with C_1 and C_2 the extinction cross sections of a single particle and a doublet (an aggregate composed of two single particles), respectively [28, 29]. In the present case for the silica in KCl solution, *F* is calculated to be 0.168 by T-matrix method [30, 31]. From our preliminary experiments, we decided the amount of HCl and KOH solution to keep the pH of suspension to 5 or 7. After the measurement, we measured the pH of the sample with 781 pH/Ion Meter (Metrohm) to check if the pH was around 5 or 7.

3. Theory

3.1 Zeta potential

The zeta potential ζ of spherical particles can be calculated from electrophoretic mobility μ with a proper theory. When $\kappa a \gg 1$ and ζ is low, where *a* is the particle radius and κ is the reciprocal of thickness of electric double layer defined by Eq. (8) for 1:1 electrolyte, we use Smoluchowski's equation [24]

$$\mu = \frac{\varepsilon_r \varepsilon_0 \zeta}{\eta} \tag{5}$$

to calculate the zeta potential, where $\varepsilon_r \varepsilon_0$ is the dielectric constant of solvent and η is the viscosity.

When particles have a zeta potential whose absolute value is larger than 50 mV, we must consider the relaxation effect. In this case, we use Ohshima's formula [25]

$$\mu = \frac{2\varepsilon_r \varepsilon_0 k_B T}{3\eta e}\left[\frac{3}{2}\tilde{\zeta} - \frac{3F}{1+F}H + \frac{1}{\kappa a}\left\{-18\left(t + \frac{t^3}{9}\right)K + \frac{15F}{1+F}\left(t + \frac{7t^2}{20} + \frac{t^3}{9}\right) - 6(1+3m_+)\left(1 - \exp\left(-\frac{\tilde{\zeta}}{2}\right)\right)G + \frac{12F}{(1+F)^2}H + \frac{9\tilde{\zeta}}{1+F}(m_+ G + m_- H) - \frac{36F}{1+F}\left(m_+ G^2 + \frac{m_-}{1+F}H^2\right)\right\}\right] \quad (6)$$

, where $\tilde{\zeta}, \kappa, H, K, F, G, t$ and $m_\pm$ are defined as

$$\tilde{\zeta} = \frac{e\zeta}{k_B T} \quad (7)$$

$$\kappa = \sqrt{\frac{2e^2 n}{\varepsilon_r \varepsilon_0 k_B T}} \quad (8)$$

$$H = \ln\frac{1 + \exp\left(\frac{\tilde{\zeta}}{2}\right)}{2} \quad (9)$$

$$K = 1 - \frac{25}{3(\kappa a + 10)}\exp\left(-\frac{\kappa a}{6(\kappa a - 6)}\tilde{\zeta}\right) \quad (10)$$

$$F = \frac{2}{\kappa a}(1 + 3m_-)\left(\exp\left(\frac{\tilde{\zeta}}{2}\right) - 1\right) \quad (11)$$

$$G = \ln\frac{1 + \exp\left(-\frac{\tilde{\zeta}}{2}\right)}{2} \quad (12)$$

$$t = \tanh\left(\frac{\tilde{\zeta}}{4}\right) \quad (13)$$

$$m_\pm = \frac{2\varepsilon_r \varepsilon_0 k_B T}{3\eta e^2}\lambda_\pm \quad (14)$$

where *e* is the elementary charge and *n* is the number concentration of 1-1 electrolyte. $\lambda_\pm$ are the drag coefficients of cations and anions which are defined by

$$\lambda_\pm = \frac{N_A e^2}{\Lambda_\pm^0} \quad (15)$$

where N_A is the Avogadro number and $\Lambda_\pm^0$ are the limiting conductances of cations and anions.

3.2 Aggregation rate constant with charge heterogeneity

We can calculate the aggregation rate constant (k_{11}) by using [14, 32]

$$k_{11} = k_s\left[2a\int_0^\infty \frac{B(h)}{(2a+h)^2}\exp\left(\frac{V(h)}{k_B T}\right)dh\right]^{-1} \quad (16)$$

$$k_s = \frac{8k_B T}{3\eta} \tag{17}$$

k_s is the Smoluchowski rate constant and h is the closest distance between sphere surfaces. $B(h)$ is the correction factor for hydrodynamic interaction and $V(h)$ is the physico-chemical interaction potential between two particles. $B(h)$ and $V(h)$ can be represented by [33]

$$B(h) \approx \frac{6\left(\frac{h}{a}\right)^2 + 13\left(\frac{h}{a}\right) + 2}{6\left(\frac{h}{a}\right)^2 + 4\left(\frac{h}{a}\right)} \tag{18}$$

$$V(h) = V_{\mathrm{vdW}}(h) + V_{\mathrm{el}}(h) \tag{19}$$

$V_{\mathrm{vdW}}(h)$ and $V_{\mathrm{el}}(h)$ are the potentials of the van der Waals attraction and the electrostatic repulsion. The $V_{\mathrm{vdW}}(h)$ between two spherical particles is given by

$$V_{\mathrm{vdW}}(h) = -\frac{A}{6}\left[\frac{2}{s^2-4} + \frac{2}{s^2} + \ln\frac{s^2-4}{s^2}\right] \tag{20}$$

where *s* is defined by

$$s = \frac{2a+h}{a} \tag{21}$$

and A is the Hamaker constant. The electrostatic repulsion is obtained by means of the Derjaguin approximation which can be represented by

$$V_{\mathrm{el}}(h) = 2\pi a\varepsilon_r\varepsilon_0\psi_d^2 \ln(1+\exp(-\kappa h)) \tag{22}$$

where ψ_d is the diffuse layer potential and, in this paper, we assume ψ_d is the same as the zeta potential. These equations assume that the average diffuse layer potential determines the electrical interaction potential. That is, surface charge heterogeneity is not considered.

A model including the effect of distribution of diffuse layer potential was used to calculate the aggregation rate more correctly [13–15]. More precisely, there are some differences between diffuse layer potential and surface potential. In this study, we assume the diffuse and surface potential are the same, and the zeta potential is the average of diffuse layer potential. Following the model, we assume the diffuse layer potential of the silica coated with lysozymes follows a normal distribution. The average and standard deviation of the diffuse layer potential of the silica with lysozymes can be determined from the experiment of electrophoretic mobility. When two particles with distributed diffuse layer potential approach to each other, the theoretical aggregation rate constant k_{11} can be given by

$$k_{11} = \int_{-\infty}^{\infty}\int_{-\infty}^{\infty} p(\psi_i,\psi_j)k(\psi_i,\psi_j)d\psi_i d\psi_j \tag{23}$$

where $k(\psi_i,\psi_j)$ can be calculated by Eq. (16) with modified $V_{\mathrm{el}}(h)$ as Eq. (24):

$$V_{\mathrm{el}}(h) = \frac{1}{2}\pi a\varepsilon_r\varepsilon_0\left[(\psi_i+\psi_j)^2\ln(1+\exp(-\kappa h)) + (\psi_i-\psi_j)^2\ln(1-\exp(-\kappa h))\right] \tag{24}$$

where ψ_i and ψ_j are the diffuse layer potential of particles *i* and *j* and the probability density function $p(\psi_i,\psi_j)$ is

$$p(\psi_i, \psi_j) = \frac{1}{\gamma\sqrt{2\pi}} \exp\left[\frac{-(\psi_i - \bar{\psi})^2}{2\gamma^2}\right] \times \frac{1}{\gamma\sqrt{2\pi}} \exp\left[\frac{-(\psi_j - \bar{\psi})^2}{2\gamma^2}\right] \quad (25)$$

where $\bar{\psi}$ and γ are the average and standard deviation of the diffuse layer potential of the silica particles with lysozymes, respectively. Here we call the calculation with Eq. (23) 1-peak model, since this model only considers the distribution of diffuse layer potential around the average and the probability density function shows one peak.

When lysozymes adsorb to silica, we can naturally imagine that positive and negative sites exist on the silica surface. Such a situation can be considered by another model, which is called 2-peak model in this paper. The 2-peak model takes account of positively charged and negatively charged patches on the surfaces. In this model, the aggregation rate constant can be given by

$$k_{11} = \int\int_{-\infty}^{\infty} f_{2A}(\psi_{S1}) f_{2B}(\psi_{S2}) k(\psi_{S1}, \psi_{S2}) d\psi_{S1} d\psi_{S2} \quad (26)$$

where $f_{2A}(\psi_{S1})$ and $f_{2B}(\psi_{S2})$ are defined by

$$f_{2A}(\psi_{S1}) = \frac{w}{\gamma_{Si}\sqrt{2\pi}} \exp\left[\frac{-(\psi_{S1} - \bar{\psi}_{Si})^2}{2\gamma_{Si}^2}\right] + \frac{1-w}{\gamma_{LYS}\sqrt{2\pi}} \exp\left[\frac{-(\psi_{S1} - \bar{\psi}_{LYS})^2}{2\gamma_{LYS}^2}\right] \quad (27)$$

$$f_{2B}(\psi_{S2}) = \frac{w}{\gamma_{Si}\sqrt{2\pi}} \exp\left[\frac{-(\psi_{S2} - \bar{\psi}_{Si})^2}{2\gamma_{Si}^2}\right] + \frac{1-w}{\gamma_{LYS}\sqrt{2\pi}} \exp\left[\frac{-(\psi_{S2} - \bar{\psi}_{LYS})^2}{2\gamma_{LYS}^2}\right] \quad (28)$$

$\bar{\psi}_{Si}, \gamma_{Si}, \bar{\psi}_{LYS}$, and γ_{LYS} are the average and the standard deviation of diffuse layer potentials of the silica and the lysozyme, respectively. *w* is the ratio of the bare silica surface to all surface and can be determined by fitting the average diffuse layer potential calculated with assumed values of *w* and the probability density function Eq. (27) with experimental zeta potentials of the silica coated with lysozymes. That is,

$$\zeta = \psi_0 = \int_{-\infty}^{\infty} \psi f(\psi) d\psi \quad (29)$$

$$f(\psi) = \frac{1-w}{\gamma_{LYS}\sqrt{2\pi}} \exp\left[\frac{-(\psi - \bar{\psi}_{LYS})^2}{2\gamma_{LYS}^2}\right] + \frac{w}{\gamma_{Si}\sqrt{2\pi}} \exp\left[\frac{-(\psi - \bar{\psi}_{Si})^2}{2\gamma_{Si}^2}\right] \quad (30)$$

where ψ_0 is the theoretical diffuse layer potential with the ratio of bare silica surface to the total surface *w*.

4. Results and discussion

4.1 Results of aggregation rate constant of bare silica

Results of measurements of aggregation rate constant *k* of bare silica particles against the KCl concentration are shown in Fig. 1. With increasing KCl concentration, the silica suspension is destabilized and the aggregation rate is enhanced. According to the DLVO theory [3, 4], the electrical double layer becomes thinner with increasing electrolyte concentration. As a result, the electrical

repulsive force between silica particles becomes weaker and the particles aggregate. When KCl concentration is below critical coagulation concentration (CCC), the aggregation rate constant changes with the change in KCl concentration. Especially at low KCl concentration such as 10 mM or lower, the thickness of electrical diffuse double layer is large. Therefore, the silica particles repel each other strongly and the aggregation rate constant is quite low. Once the KCl concentration exceeds CCC, *k* remains the constant value k_f. The CCC changes with pH because the charge density and zeta potential of silica particles change with pH. At pH 7, the absolute value of zeta potential of silica is higher than that at pH 5 (Fig. 2) [16]. Therefore, the repulsive force between silica particles is weaker at pH 5, so the CCC is lower. In the rapid aggregation regime, the values of *k* at different pH are the same because electrical repulsive force is screened and the aggregation rate is determined by the van der Waals force and the collision frequency by Brownian motion. It is often pointed out that the aggregation rate of silica nanoparticles becomes extremely low at low pH [12, 16], or when the particles are too small [34]. This anomaly stable silica is not the case for the present study probably because of the heat treatment and larger size. The aggregation rate constant in the rapid aggregation regime (k_f in Fig. 1) is $(2.2 \pm 0.6) \times 10^{-18}$ m^3/s, which is close to the previous study, while the rate constant is smaller than the prediction of DLVO theory [16].

4.2 Experimental results of adsorbed amount of lysozyme and zeta potential of silica

The adsorbed amount of lysozyme on silica at 1 mM and 10 mM KCl are shown in Fig. 2. According to Fig. 2, we can see that the adsorbed amount changes drastically with the change of pH, but show less dependence on KCl concentration. As for other materials such as linear polymers and surfactants, the maximum adsorbed amount increases with the increase in electrolyte concentration [37-39], while the adsorption of anionic dye on oppositely charged surface shows that the adsorbed amount decreases with the increase in electrolyte concentration [40].

About the dependence of adsorbed amount on pH and on KCl concentration, we consider that the concept of a three-body random sequential adsorption (RSA) model can qualitatively explain the results of our study [36]. According to the two-body RSA model, the maximum adsorbed amount of particles on a substrate is determined by the lateral electrical repulsion between adsorbed particles when the substrate surface is weakly charged and particles are large. The increase in salt concentration and the decrease in absorbed particle charge reduce the lateral repulsion and thus the maximum adsorbed amount increases. When the substrate surface is highly charged and the adsorbed particles are small, the three-body RSA model suggests that the lateral repulsion of adsorbed particles decreases due to the additional screening by the diffuse double layer developed from the oppositely charged substrate surface. As a result, the maximum adsorbed amount increases with increasing the substrate surface charge and the dependence of the maximum adsorbed amount on salt concentration becomes weaker.

In our study, the thickness of electrical diffuse double layer is about 3 nm at 10 mM KCl and 10 nm at 1 mM KCl. The thickness of diffuse double layer is close to or larger than the lysozyme size. Therefore, the explanation of three-body RSA model can work for our system. The maximum adsorbed amount of

lysozyme is affected not only by the lateral repulsion between adsorbed lysozymes with positive charge but also by the negative charge of silica surface. For the pH dependence, when pH changes from 5 to 7, the charge of silica increases [12] and the charge of lysozyme decreases [23]. According to the three-body RSA model, the range of the repulsive interaction between adsorbed lysozymes becomes smaller and the maximum adsorbed amount increases. Similar experimental results are reported by previous studies [22, 35]. For the KCl concentration dependence, when KCl concentration is low and the lysozyme charge is high, the range of the repulsive interaction between adsorbed lysozymes becomes larger and thus the maximum adsorbed amount decreases. However, the oppositely charged silica surface reduces the lateral repulsion and increases the adsorbed amount compared to the condition that only the interaction between lysozymes is taken account. Therefore, we cannot see obvious effect of KCl concentration on the adsorbed amount in our study. A part of the data of adsorption of positively charged poly(amido amine) (PAMAM) dendrimers on negatively charged silica surfaces shows similar weak dependence on salt concentration in a rather narrow range of salt concentration [36].

Also, according to Kubiak-Ossowska et al. [41], the hydrophobic interaction may play an additionally important role in adsorption process because of the hydrophilic and hydrophobic groups of lysozymes.

The adsorbed amount affects the zeta potential of lysozyme-coated silica. The zeta potential of silica with lysozymes at 1 mM and 10 mM KCl are shown in Fig. 3. The results of zeta potential against the adsorbed amount are given in Fig. 4. With increasing the lysozyme dose, the zeta potential of silica increases from negative to 0 and reverses to positive. Above the point of zero zeta potential, the zeta potential changes slightly and reaches a plateau. This trend of the zeta potential can be explained by the adsorption of positively charged lysozymes on the surface of the silica bearing negative charges. The plateau zeta potential corresponds to the almost saturation of the adsorption. We can also see a change of point of zero zeta potential with the changing of KCl concentration, and a theoretical so-called 3D model [42, 43] is proposed to describe the change of zeta potential of the surface covered with particles. According to 3D model, because the charge and zeta potential of lysozyme and silica particles are influenced by KCl concentration, the change of the point of zero zeta potential with KCl concentration is possible. There are also some previous studies reporting that the point of zero zeta potential or zero EPM depends on the concentration of simple 1:1 electrolytes [6, 44-47]. Therefore, we think that the point of zero zeta potential can change with the KCl concentration. Future studies applying the 3D model to silica-lysozyme systems may provide further insights.

4.3 Experimental results of aggregation rate constant of silica with lysozyme

Aggregation rate constant against the mass ratio of lysozyme to silica are shown in Fig. 5. The solid lines in Fig. 5 are the fast aggregation rate constant of the bare silica k_f and is drawn to compare the maximum aggregation rate in the presence of lysozymes. When lysozyme is added, with increasing the lysozyme dose, the rate increases, passes through the maximum, and decreases. The aggregation rate reaches the maximum around the point of zero zeta potential. We found that the maximum aggregation rates in the presence of lysozymes at both pH 5 and 7 are higher than k_f, indicating that the lysozyme

has an effect to increase the aggregation rate of silica. The adsorption of lysozyme increases the minimum separation distance between two silica particles. This may make the van der Waals force smaller. Therefore, we think that the increase of the maximum aggregation rate is not due to the change of the van der Waals forces. Also, the maximum of aggregation rate constant at the point differing from zero zeta potential is found. Similar results are shown in a previous study [47] reporting that the point of maximum aggregation rate does not coincide with the point of zero zeta potential.

We consider that the reason of increase of aggregation rate is the heterogeneities on the silica surface. When lysozymes adsorb on the silica surface below full surface coverage, positively charged patches appear and not only the van der Waals force but also the attractive electrical force between the positively charged patches and the negatively charged bare surface of the other silica particle acts. That is, the charge-patch electrical attractive force accelerates the aggregation rate [48]. The maximum aggregation rate becomes lower at 1 mM than that at 10 mM. This trend cannot be explained by only the attractive double layer force, since the attractive double layer force is strong at low salt concentration [6, 8, 9, 49]. At point of zero zeta potential, there are not only the attractive force between patches and bare surface but also the repulsive force between patches themselves. At low KCl concentration, the repulsive forces increase too. This may make the maximum aggregation rate constant lower at low KCl concentration than that at high KCl concentration. Also, at pH 7 and 1 mM KCl, the maximum of aggregation rate constant is not at point of zero zeta potential, so the effect of electrical repulsive force of electrical double layers may reduce the maximum aggregation rate. The region of the fastest rate is wider for high KCl concentration. This is simply because the electrostatic repulsion is screened at high ion concentration as expected by DLVO theory [3, 4].

Because there are binding sites on opposite sides of the lysozyme [10, 50], the bridging of silica particles by lysozymes is also possible and can enhance the attachment efficiency of aggregation. This mechanism and the charge-patch interaction can work when the surface is not fully saturated with lysozyme. The maximum rate appeared at unsaturated doses, therefore these mechanisms are plausible for our result. The detailed mechanism of the interactions between silica and lysozymes is unclear at this moment, therefore, the dependency on pH and salt concentration is not predictive. We still need further studies for this point.

4.4 Comparison of experiment to model calculation

As introduced in the theory part, we use the 1-peak model, the 2-peak model, and the DLVO theory to calculate aggregation rates theoretically. By fitting the data in the absence of lysozyme in Fig. 1 into the DLVO theory, we assume the Hamaker constant around 1.0×10^{-21} J, and the average and coefficient of variation of diffuse layer potential of the silica and the lysozyme are obtained from experimental results of their electrophoresis.

A comparison of aggregation rate constants among the experiments, the 2-peak model, the 1-peak model, and the DLVO theory is shown in Fig. 6. In Fig. 6(a) for pH 5 at 10 mM, the calculation with 2-peak model is close to the experimental results at low dose of the lysozyme. However, above the point

of zero zeta potential, values by the 2-peak model are much higher than the experiment. When the dose is higher than point of zero zeta potential, more lysozymes are adsorbed on the surface of silica and thus a positively charged lysozyme layer is effectively formed. As a result, the attraction originating from effects of charge heterogeneity becomes weaker. In this study, the zeta potential after charge reversal become plateau at about 10 mV. Therefore, we cannot verify the aggregation rate constant at the zeta potential higher than 10 mV. If the zeta potential increases further, we expect that the plots of *k* are close to the prediction by the DLVO and 1-peak model.

In Fig. 6(b), the calculation of 1-peak model is close to the experimental results below the point of zero zeta potential. Comparing Fig. 6(b) with (a), we see that the plots approach to the prediction by 1-peak model. Figure 2 shows that the adsorbed amount at pH 7 is much more than that at pH 5. When the adsorbed amount increases, lysozymes form a homogeneously charged layer and weakens the effect of charge heterogeneity. Even though the distribution of diffuse layer potential contributes to the aggregation process, the effect of charge heterogeneity almost disappears. Another reason of redispersion of silica is considered to be the steric stabilization. Lysozymes adsorb on the surface of silica and make the surface rough. When the adsorption of lysozymes is saturated, further adsorption of lysozymes is inhibited. In turn, the silica effectively covered or saturated by lysozymes cannot easily aggregate. Therefore, silica particles re-disperse more quickly than the prediction of DLVO theory and 1-peak model because of the steric repulsive forces.

We see that the maximum of the aggregation rate constant is not at the point of zero zeta potential in Fig. 6((c) and (d)). These phenomena confirmed by experiment can be seen only by 2-peak model. However, there are also some problems that the prediction by 2-peak model does not quantitatively agree with the experiment.

We also note the asymmetry of *k* against the point of zero zeta potential in Fig. 6. The prediction by DLVO theory and 1-peak model is symmetrical around the point of zero zeta potential. In contrast, the 2-peak model shows asymmetry, while the asymmetry is too much. In Fig. 6((a) and (b)), when the adsorbed amount is low below the point of zero zeta potential, the *k* grows gradually even though the zeta potential is high. Above the point of zero zeta potential, the zeta potential does not change obviously, but the *k* falls rapidly because of the disappearance of charge-patch force and the appearance of steric force originating from lysozyme-lysozyme interaction. The change of effectiveness of charge heterogeneity before and after point of zero zeta potential makes the plots of *k* asymmetrical.

Even though the prediction by 2-peak model does not quantitatively agree with the experiment, only the 2-peak model describe the asymmetry and especially the fastest area out of point of zero zeta potential. Furthermore, the experimental fact that the maximum of aggregation rate constant is not at the point of zero zeta potential can be predicted only by 2-peak model. In this sense, the 2-peak model including heterogeneity of positive and negative charges can somehow describe the aggregation behavior of the lysozyme-coated silica particles. Further improvement can be expected by properly considering realistic charge heterogeneity and the effect of the surface coverage of lysozymes on the silica.

5. Conclusion

To clarify the effect of lysozymes on the charging and aggregation of silica particles, we examined the zeta potential and the aggregation rate constant of silica particles in the presence of lysozymes. The measured rate constants were compared with the theoretical values predicted by the 2-peak model, the 1-peak model, and the classical DLVO theory. While the charge neutralization and charge stabilization are significant, additional interaction mechanisms need to be taken into consideration. We suggest charge heterogeneity and steric interaction as such additional mechanisms. The experimental aggregation rate constant is close to the theoretical value predicted by the 2-peak model, which is proposed to quantify the effect of the charge heterogeneity, when the adsorbed amount is quite low. This supports the hypothesis of the existence of the effect of charge heterogeneity. The charge heterogeneity is effective to promote the aggregation of silica particles at the low adsorbed amount. At the high adsorbed amount, the formation of the effectively saturated lysozyme layer inhibits aggregation. Further improvement should be needed to consider realistic charge heterogeneity and the effect of the surface coverage of lysozyme on the silica.

Acknowledgements This work was financially supported by JSPS KAKENHI (15H04563 and 16H06382).

Conflict of interest The authors declare that they have no conflict of interest.

References

1. Canham LT (2007) Nanoscale semiconducting silicon as a nutritional food additive. Nanotechnology 18:185704. doi: 10.1088/0957-4484/18/18/185704
2. Vallet-Regí M, Ruiz-González L, Izquierdo-Barba I, González-Calbet JM (2006) Revisiting silica based ordered mesoporous materials: medical applications. J Mater Chem 16:26. doi: 10.1039/b509744d
3. Derjaguin B V (1941) Theory of the Stability of Strongly Charged Lyophobic Sols and of the Adhesion of Strongly Charged Particles in Solutions of Electrolytes. Acta Physicochim USSR 14:633–662.
4. Verwey EJW, Overbeek JTG (1955) Theory of the Stability of Lyophobic Colloids. J Colloid Sci 10:224–225.
5. Nishiya M, Sugimoto T, Kobayashi M (2016) Electrophoretic mobility of carboxyl latex particles in the mixed solution of 1:1 and 2:1 electrolytes or 1:1 and 3:1 electrolytes: Experiments and modeling. Colloids Surfaces A Physicochem Eng Asp 504:219–227. doi: 10.1016/j.colsurfa.2016.05.045
6. Lin W, Galletto P, Borkovec M (2004) Charging and aggregation of latex particles by oppositely charged dendrimers. Langmuir 20:7465–7473. doi: 10.1021/la049006i
7. Kobayashi M, Yuki S, Adachi Y (2016) Effect of anionic surfactants on the stability ratio and electrophoretic mobility of colloidal hematite particles. Colloids Surfaces A Physicochem Eng Asp 510:190–197. doi: 10.1016/j.colsurfa.2016.07.063
8. Adachi Y, Feng L, Kobayashi M (2015) Kinetics of flocculation of polystyrene latex particles in the mixing flow induced with high charge density polycation near the isoelectric point. Colloids Surfaces A Physicochem Eng Asp 471:38–44. doi: 10.1016/j.colsurfa.2015.02.011
9. Szilagyi I, Trefalt G, Tiraferri A, et al (2014) Polyelectrolyte adsorption, interparticle forces, and colloidal aggregation. Soft Matter 10:2479–502. doi: 10.1039/c3sm52132j
10. Bharti B, Meissner J, Klapp SHL, Findenegg GH (2014) Bridging interactions of proteins with silica nanoparticles: the influence of pH, ionic strength and protein concentration. Soft Matter 10:718. doi: 10.1039/C3SM52401A
11. Lerche D, Sobisch T (2014) Evaluation of particle interactions by in situ visualization of separation behaviour. Colloids Surfaces A Physicochem Eng Asp 440:122–130. doi: 10.1016/j.colsurfa.2012.10.015
12. Kobayashi M, Juillerat F, Galletto P, et al (2005) Aggregation and charging of colloidal silica particles: effect of particle size. Langmuir 21:5761–5769. doi: 10.1021/la046829z
13. Kihira H, Ryde N, Matijević E (1992) Kinetics of heterocoagulation. Part. 2—The effect of the discreteness of surface charge. J Chem Soc, Faraday Trans 88:2379–2386.
14. Schudel M, Behrens SH, Holthoff H, et al (1997) Absolute Aggregation Rate Constants of Hematite Particles in Aqueous Suspensions : A Comparison of Two Different Surface Morphologies. 253:241–253.
15. Cooper WD (1972) Coagulation of polydisperse colloidal systems. Kolloid-Zeitschrift und

Zeitschrift für Polym 250:38–45. doi: 10.1007/BF01508209

16. Kobayashi M, Skarba M, Galletto P, et al (2005) Effects of heat treatment on the aggregation and charging of Stober-type silica. J Colloid Interface Sci 292:139–147. doi: 10.1016/j.jcis.2005.05.093
17. Jachimska B, Kozłowska A, Pajor-Świerzy A (2012) Protonation of lysozymes and its consequences for the adsorption onto a mica surface. Langmuir 28:11502–11510. doi: 10.1021/la301558u
18. Kim JY, Ahn SH, Kang ST, Yoon BJ (2006) Electrophoretic mobility equation for protein with molecular shape and charge multipole effects. J Colloid Interface Sci 299:486–492. doi: 10.1016/j.jcis.2006.02.003
19. Tan WF, Koopal LK, Weng LP, et al (2008) Humic acid protein complexation. Geochim Cosmochim Acta 72:2090–2099. doi: 10.1016/j.gca.2008.02.009
20. Norde W, Gonzalez FG, Haynes CA (1995) Protein adsorption on polystyrene latex particles. Polym Adv Technol 6:518–525.
21. Kuehner DE, Engmann J, Fergg F, et al (1999) Lysozyme net charge and ion binding in concentrated aqueous electrolyte solutions. J Phys Chem B 103:1368–1374. doi: 10.1021/jp983852i
22. Bharti B, Meissner J, Findenegg GH (2011) Aggregation of silica nanoparticles directed by adsorption of lysozyme. Langmuir 27:9823–9833. doi: 10.1021/la201898v
23. Yamaguchi A, Kobayashi M (2016) Quantitative evaluation of shift of slipping plane and counterion binding to lysozyme by electrophoresis method. Colloid Polym Sci 1–8. doi: 10.1007/s00396-016-3852-4
24. Smoluchowski M V. (1903) Contribution to the theory of electro-osmosis and related phenomena. Bull Int Acad Sci Cracovie 3 184–199.
25. Ohshima H, Healy TW, White LR (1983) Approximate analytic expressions for the electrophoretic mobility of spherical colloidal particles and the conductivity of their dilute suspensions. J Chem Soc Faraday Trans 2 79:1613–1628. doi: 10.1039/F29837901613
26. Smoluchowski M V. (1916) Three discourses on diffusion, Brownian movements, and the coagulation of colloid particles. Phys Z Sowjet 17:557–571.
27. Smoluchowski M V. (1917) Mathematical Theory of the Kinetics of the Coagulation of Colloidal Solutions. Z Phys Chem 92:129–168.
28. Sun Z, Liu J, Xu S (2006) Study on improving the turbidity measurement of the absolute coagulation rate constant. Langmuir 22:4946–4951. doi: 10.1021/la0602160
29. Lichtenbelt JWT, Ras HJMC, Wiersema PH (1974) Turbidity of coagulating lyophobic sols. J Colloid Interface Sci 46:522–527. doi: 10.1016/0021-9797(74)90063-0
30. Mishchenko MI, Travis LD, Mackowski DW (1996) T-matrix computations of light scattering by nonspherical particles: A review. J Quant Spectrosc Radiat Transf 55:535–575. doi: 10.1016/0022-4073(96)00002-7
31. Kobayashi M, Ishibashi D (2011) Absolute rate of turbulent coagulation from turbidity measurement. Colloid Polym Sci 289:831–836. doi: 10.1007/s00396-011-2388-x
32. Russel WB, Saville DA, Schowalter WR (1989) Colloidal Dispersions. Cambridge University Press,

Cambridge

33. Honig EP, Roebersen GJ, Wiersema PH (1971) Effect of hydrodynamic interaction on the coagulation rate of hydrophobic colloids. J Colloid Interface Sci 36:97–109. doi: 10.1016/0021-9797(71)90245-1
34. Higashitani K, Nakamura K, Shimamura T, et al (2017) Orders of Magnitude Reduction of Rapid Coagulation Rate with Decreasing Size of Silica Nanoparticles. Langmuir acs.langmuir.7b00932. doi: 10.1021/acs.langmuir.7b00932
35. Kumar K, Aswal V, et al (2014) pH-Dependent Interaction and Resultant Structures of Silica Nanoparticles and Lysozyme Protein. Langmuir 30:1588-1598.
36. Cahill B, Papastavrou G, Koper G, et al (2008) Adsorption of Poly (amido amine) (PAMAM) Dendrimers on Silica: Importance of Electrostatic Three-Body Attraction. Langmuir 24:465-473
37. Pham T, Kobayashi M, Adachi Y (2014) Adsorption of Polyanion onto Large Alpha Alumina Beads with Variably Charged Surface. Advances in Physical Chemistry.
38. Goloub T, Koopal L, Bijsterbosch B, et al (1996) Adsorption of Cationic Sur factants on Silica . Surface Charge Effects. Langmuir 12:3188-3194
39. Pham T, Kobayashi M, Adachi Y (2015) Adsorption of anionic surfactant sodium dodecyl sulfate onto alpha alumina with small surface area. Colloid and Polymer Science 293:217-227
40. Pham T, Kobayashi M, Adachi Y (2015) Adsorption characteristics of anionic azo dye onto large α -alumina beads. Colloid and Polymer Science 293:1877-1886.
41. Kubiak-Ossowska K, Cwieka M, et al (2015) Lysozyme adsorption at a silica surface using simulation and experiment: effects of pH on protein layer structure. Physical Chemistry Chemical Physics 17.37: 24070-24077
42. Adamczyk Z, Warszynski P, Zembala M (1999) Influence of adsorbed colloid particles on streaming potential. Bulletin of the Polish Academy of Science 47:239-258
43. Sadowska M, Adamczyk Z, Nattich-Rak M (2014) Mechanism of nanoparticle deposition on polystyrene latex particles. Langmuir 30:692-699
44. Michna A, Adamczyk Z, Kubiak K, Jamrozy K (2014) Formation of PDADMAC monolayers evaluated in situ by QCM and streaming potential measurements. Journal of Colloid and Interface science 428:170-177
45. Sofinska K, Adamczyk Z, Kujda M, Nattich-Rak M (2013) Recombinant albumin monolayers on latex particles. Langmuir 30:250-258
46. Moussa M, Caillet C, Town RM, Duval JFL (2015) Remarkable electrokinetic features of charge-stratified soft nanoparticles: Mobility reversal in monovalent aqueous electrolyte. Langmuir 31:5656-5666
47. Yu W, Bouyer F, Borkovec M (2001) Polystyrene sulfate latex particles in the presence of poly (vinylamine): absolute aggregation rate constants and charging behavior. Journal of Colloid and Interface Science 241:392-399
48. Gregory J (1973) Rates of flocculation of latex particles by cationic polymers. J Colloid Interface

Sci 42:448–456. doi: 10.1016/0021-9797(73)90311-1
49. Lin W, Kobayashi M, Skarba M, et al (2006) Heteroaggregation in binary mixtures of oppositely charged colloidal particles. Langmuir 22:1038–1047. doi: 10.1021/la0522808
50. Kubiak K, Mulheran PA (2009) Molecular dynamics simulations of hen egg white lysozyme adsorption at a charged solid surface. The Journal of Physical Chemistry B 113:12189-12200

Figure captions

Fig. 1 The aggregation rate constant of bare silica against KCl concentration. Symbols denote the aggregation rate constant *k* at pH 5 and 7. The solid line denotes the aggregation rate constant in fast aggregation regime (k_f).

Fig. 2 Adsorbed amount of lysozyme against the mass ratio of lysozyme to silica. Symbols denote the adsorbed amount. The solid line denotes the adsorbed amount when all the added lysozymes adsorb on the silica surface. Error bars denote the standard deviations of adsorbed amount.

Fig. 3 Zeta potentials of silica in the presence of lysozyme at 1 mM and 10 mM KCl at pH 5 (a) and at pH 7 (b). The silica concentration is 0.1 g/L. Symbols denote the zeta potential.

Fig. 4 Zeta potential of silica against the adsorbed amount of lysozyme. Symbols denote the adsorbed amount of lysozyme.

Fig. 5 Aggregation rate constant against the mass ratio of lysozyme to silica at 1 mM and 10 mM KCl at pH 5 (a) and at pH 7 (b). The silica concentration is 0.1 g/L. Symbols denote the aggregation rate constants. Solid lines denote the rapid aggregation rate constant k_f of bare silica. Vertical dashed lines and dotted lines denote point of zero zeta potential at KCl concentration of 10 mM and 1 mM, respectively.

Fig. 6 Aggregation rate constant *k* of experiment (○), 2-peak model (- - - -), 1-peak model (……) and DLVO theory (— —). The solid line denotes the aggregation rate constant in fast aggregation regime (k_f) without lysozyme. The KCl concentration and pH are: (a) 10 mM, pH 5; (b) 10 mM, pH 7; (c) 1 mM, pH 5; (d) 1 mM, pH 7.

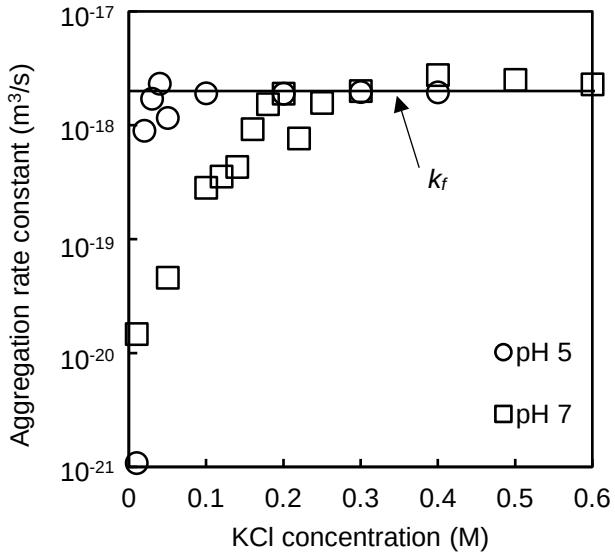

Fig. 1 The aggregation rate constant of bare silica against KCl concentration. Symbols denote the aggregation rate constant k at pH 5 and 7. The solid line denotes the aggregation rate constant in fast aggregation regime (k_f).

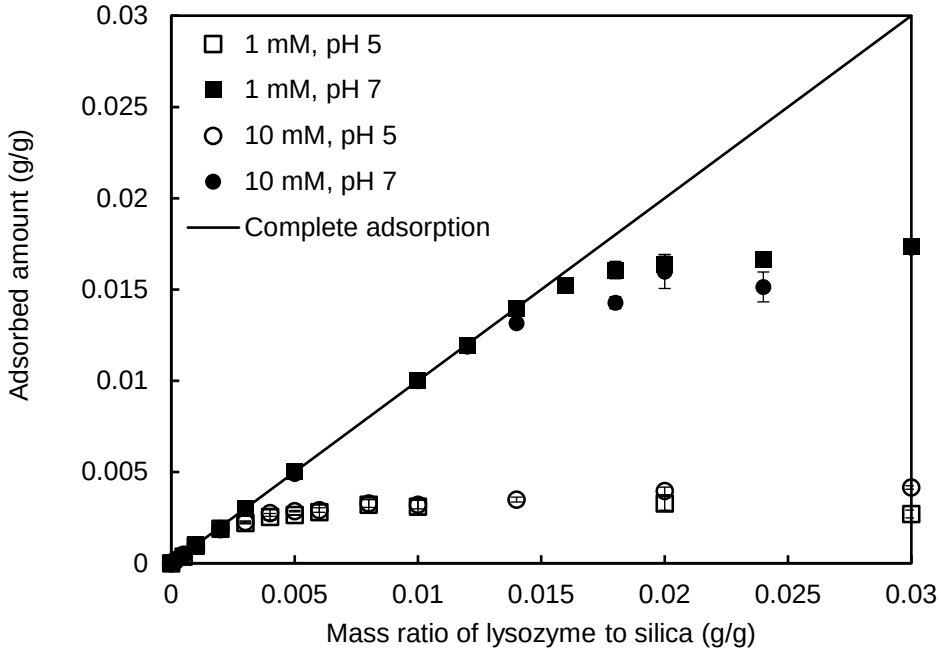

Fig. 2 Adsorbed amount of lysozyme against the mass ratio of lysozyme to silica. Symbols denote the adsorbed amount. The solid line denotes the adsorbed amount when all the added lysozymes adsorb on the silica surface. Error bars denote the standard deviations of adsorbed amount.

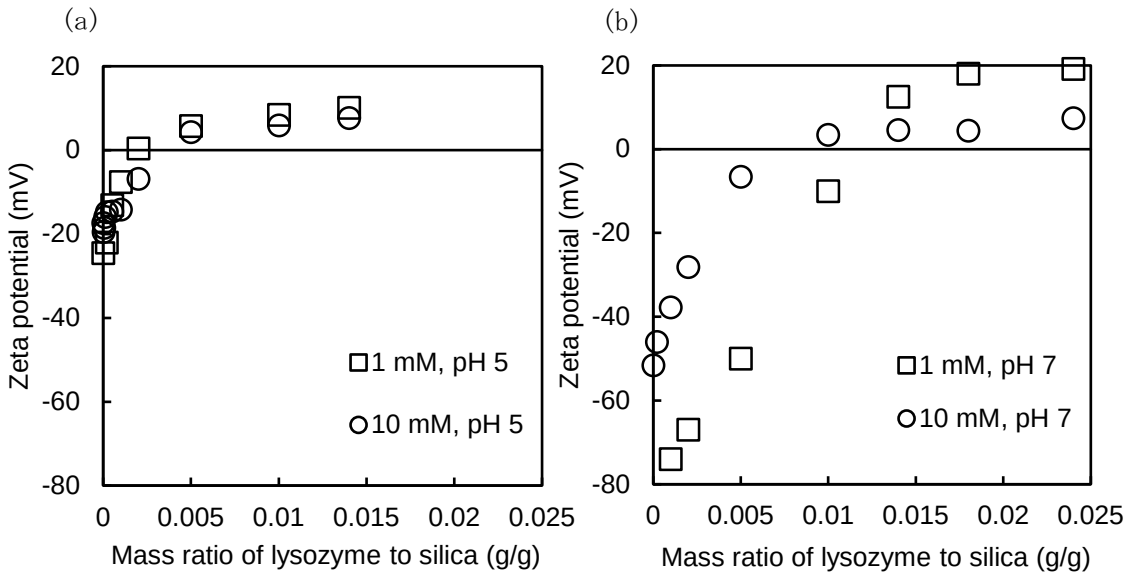

Fig. 3 Zeta potentials of silica in the presence of lysozyme at 1 mM and 10 mM KCl at pH 5 (a) and at pH 7 (b). The silica concentration is 0.1 g/L. Symbols denote the zeta potential.

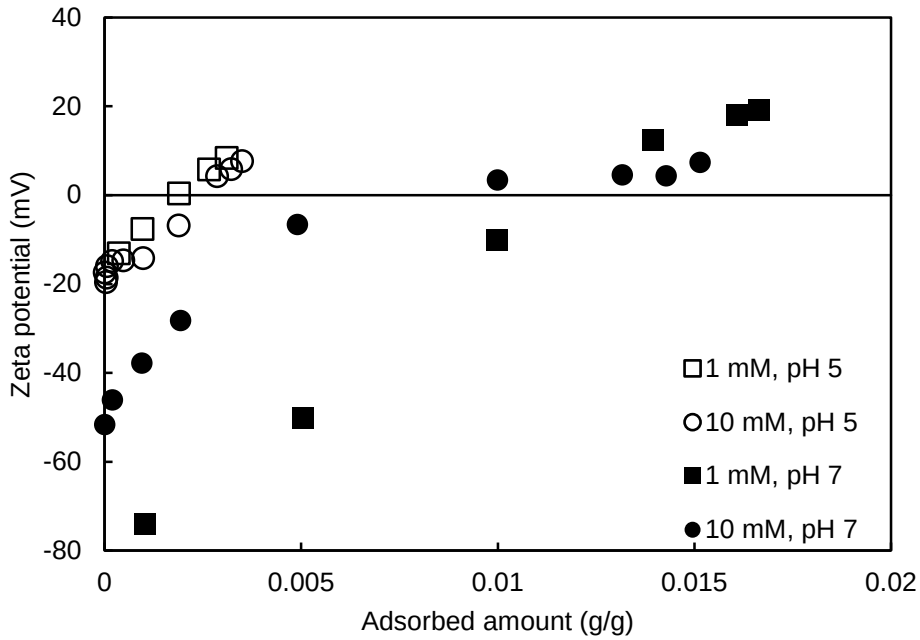

Fig. 4 Zeta potential of silica against the adsorbed amount of lysozyme. Symbols denote the adsorbed amount of lysozyme.

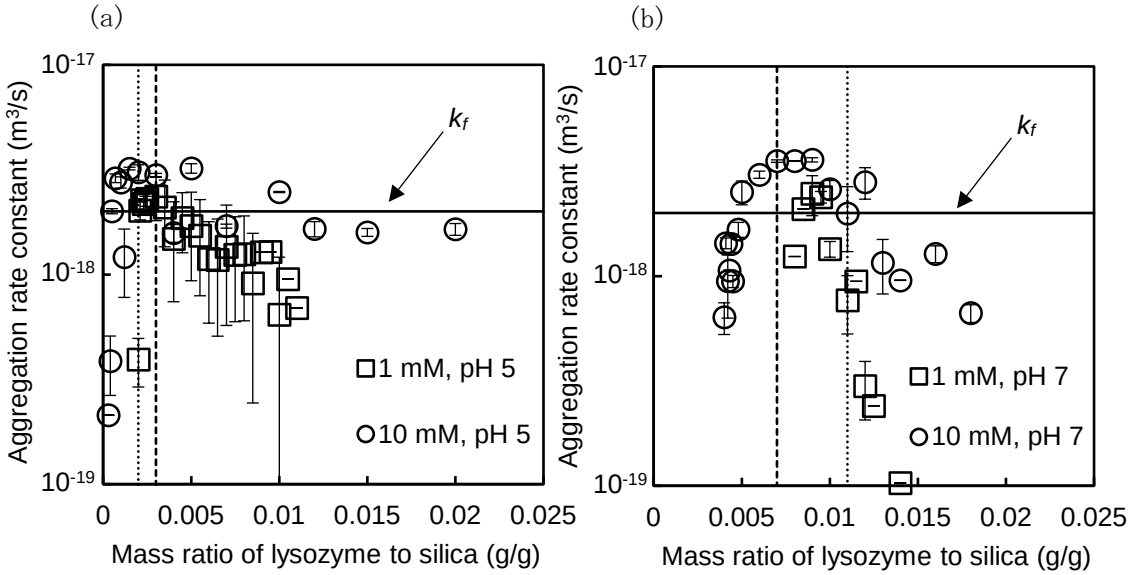

Fig. 5 Aggregation rate constant against the mass ratio of lysozyme to silica at 1 mM and 10 mM KCl at pH 5 (a) and at pH 7 (b). The silica concentration is 0.1 g/L. Symbols denote the aggregation rate constants. Solid lines denote the rapid aggregation rate constant k_f of bare silica. Vertical dashed lines and dotted lines denote point of zero zeta potential at KCl concentration of 10 mM and 1 mM, respectively.

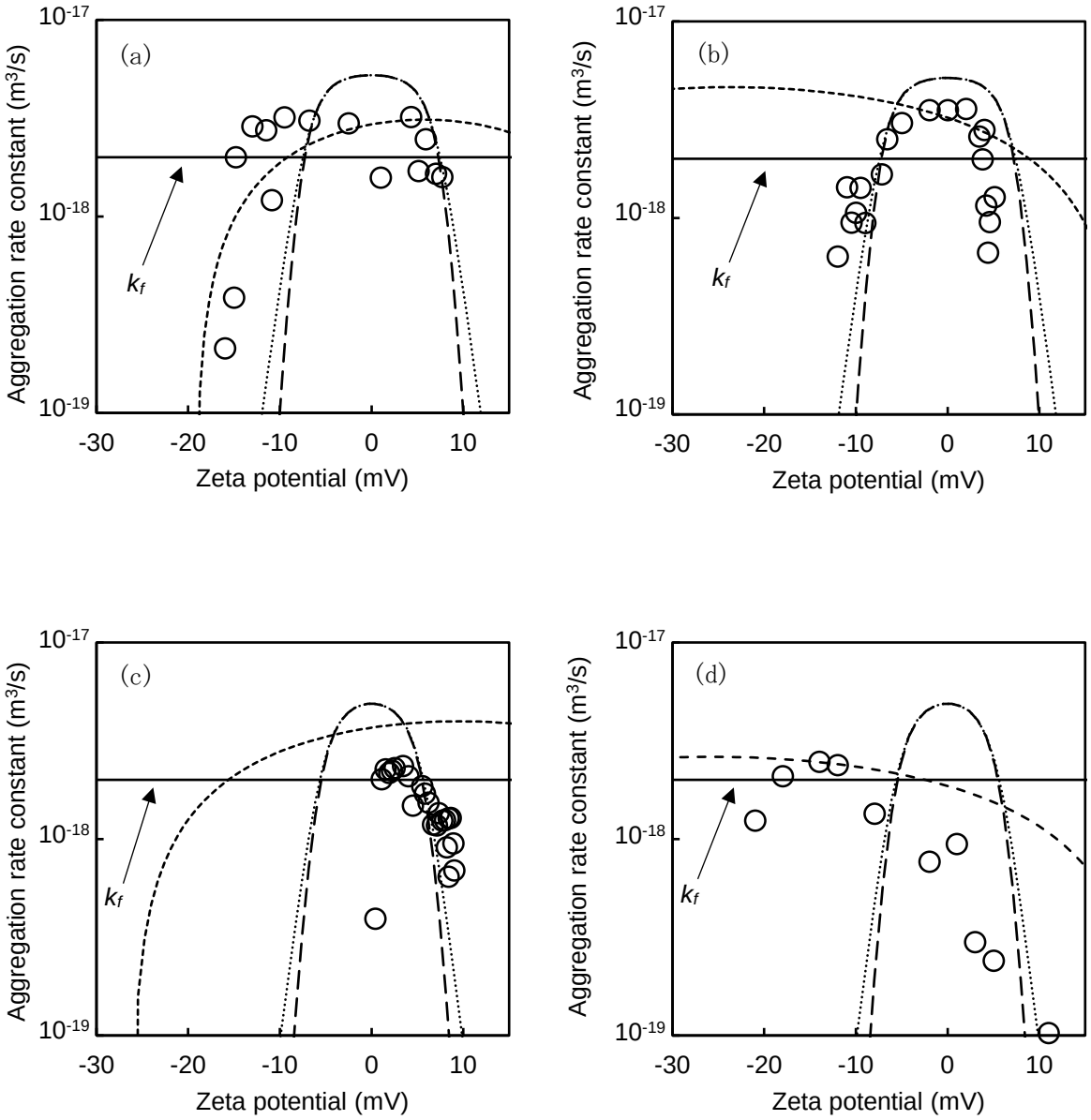

Fig. 6 Aggregation rate constant *k* of experiment (○), 2-peak model (- - - -), 1-peak model (……) and DLVO theory (— —). The solid line denotes the aggregation rate constant in fast aggregation regime (k_f) without lysozyme. The KCl concentration and pH are: (a) 10 mM, pH 5; (b) 10 mM, pH 7; (c) 1 mM, pH 5; (d) 1 mM, pH 7.